Oxidation of Metals, Vol. 3, No. 2, 1971

A Comparison of the Oxidation Behavior of Fe–Cr–Al, Ni–Cr–Al, and Co–Cr–Al Alloys

F. H. Stott,* G. C. Wood,* and M. G. Hobby†

Received June 17, 1970—Revised September 2, 1970

The main modes of isothermal oxidation of Fe–Cr–Al, Ni–Cr–Al, and Co–Cr–Al Alloys, containing 10–15% or 26–30% Cr and 0.9–1.3% or 4.3–5.7% Al, in oxygen at 1000 and 1200°C are summarized. Where protective α-Al_2O_3 scales always predominate, their ease of formation is in the order Fe–Cr–Al > Ni–Cr–Al > Co–Cr–Al. However, where catastrophic breakaway is possible, Ni–Cr–Al gives the most reliably protective scales, whereas Co–Cr–Al produces the most generally distributed breakaway or initially nonprotective scales, and Fe–Cr–Al the most locally catastrophic breakaway. The oxidation behavior is discussed in terms of the pertinent alloy and oxide parameters.

INTRODUCTION

As the prevailing conditions in many practical applications become more severe, it is increasingly necessary to rely upon alloys giving essentially α-Al_2O_3 rather than Cr_2O_3 as the protective scale. The most widely used materials in this category are those based on the alloy systems Fe–Cr–Al, Ni–Cr–Al, and Co–Cr–Al. There have been several fundamental studies of the Fe–Cr–Al system but consideration of the Ni–Cr–Al and Co–Cr–Al systems in the open literature has been minimal. These studies are not considered in the present paper, other than to note that detailed sequential examinations of scale structure as a function of time have been largely lacking.

Such investigations have recently been completed by the present authors,[1,2] using mainly isothermal kinetic measurements, optical and

*Corrosion Science Division, Department of Chemical Engineering, University of Manchester Institute of Science and Technology, Manchester, England.
†Present address: Culham Laboratories, Abingdon, Berkshire, England.

scanning electron microscopy, electron probe microanalysis, and, in specific cases, x-ray diffraction. The overall scaling behavior is relatively complicated. Nevertheless, it appeared appropriate to compare all the various modes of behavior in a short general paper, as a prelude to further detailed papers dealing with the specific behavior of certain groups of alloys.

EXPERIMENTAL PROCEDURE

The alloys listed in Table I were cut into samples approximately 2.0 × 0.5 × 0.050 cm. These were then electropolished or lightly abraded prior to direct entry into silica-spring thermobalances, containing pure flowing oxygen at 1 atm pressure, previously preheated to 1000 or 1200°C. There were minor differences in behavior determined by the surface finish, but these did not affect the overall pattern significantly. In a few of the Fe–Cr–Al runs, the oxygen was saturated with the volatile species from Cr_2O_3, by inserting a Cr_2O_3 crucible in the base of the furnace.

After cooling over 15 min at the end of the run, the specimens were studied by the now conventional techniques of optical microscopy and electron probe microanalysis of sections. Fractured samples of scale and alloy were examined by scanning electron microscopy, while a few scales were studied by powder x-ray diffraction methods.

Table I. Weight Gains After Oxidizing Fe–Cr–Al, Ni–Cr–Al, and Co–Cr–Al Alloys for 25 hr at 1000 or 1200°C

Alloy composition (wt.%)	Weight gain (mg/cm^2)		Atmosphere
	1000°C	1200°C	
Fe–12.9Cr–1.3Al	1.5 to 2	7 to 12	$Cr_2O_3 + O_2$ (1200°C) O_2 (1000°C)
Fe–26.1Cr–0.9Al	1 to 2	4 to 5	$Cr_2O_3 + O_2$
Ni–15.1Cr–1.1Al	0.45	1.4	O_2
Ni–28.8Cr–1.0Al	0.6	2.2	O_2
Co–10.0Cr–1.0Al	55	75 (6 hr only)	O_2
Co–15.0Cr–1.0Al	40	60 (6 hr only)	O_2
Co–30.0Cr–1.0Al	3	10	O_2
Fe–11.5Cr–5.7Al	0.2	1 to 5	O_2
Fe–27.8Cr–4.9Al	0.15 to 0.25	0.5 to 1	O_2
Ni–14.8Cr–4.4Al	0.35	0.7	O_2
Ni–28.7Cr–4.3Al	0.4	0.8	O_2
Co–15.0Cr–4.5Al	0.3 to 1.4	1 to 18	O_2
Co–28.0Cr–4.5Al	0.2 to 0.6	0.7 to 0.9	O_2

RESULTS

Although oxidation always occurred slowly at a declining rate, except when nodular growth occurred from the start of a run or after breakaway of an initially protective scale, the kinetics did not obey any very simple overall relationships. Consequently the weight gain after 25 hr exposure has been used as an initial, quantitative criterion of comparison (Table I). Kinetic evidence for breakaway was obtained for most of the alloys, although in some cases the sudden weight gains were relatively small as healing layers rapidly re-formed. The types of growth relationship obeyed by these alloys

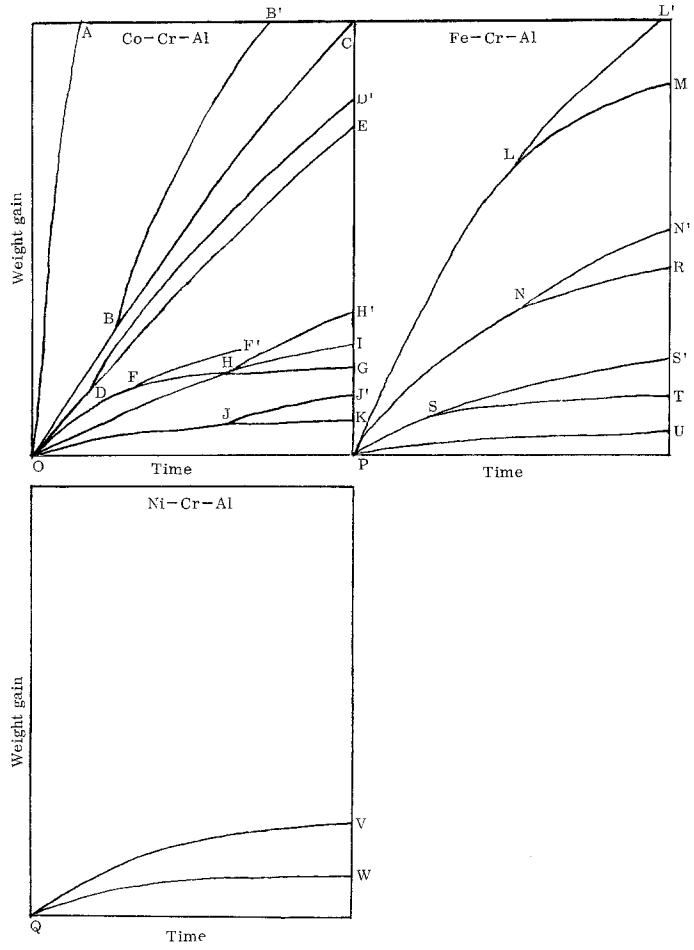

Fig. 1. Schematic growth curves for the oxidation of Co–Cr–Al, Fe–Cr–Al, and Ni–Cr–Al alloys at 1000 and 1200°C. The total oxidation period in each case was 24 hr.

in the composition range investigated are shown schematically in Fig. 1. The actual shapes and positions depended on the alloy and the oxidizing conditions, but the relative positions for any given set of alloys in the three systems are approximately correct at both 1000 and 1200°C. The total weight gains listed in Table I permit a more quantitative estimate of the exact positions of each curve for individual alloys.

Co–Cr–Al alloys containing 10 to 15% Cr and 1% Al oxidized very rapidly at 1000°C and 1200°C (curve OA), following a parabolic law reasonably closely. Co–30%Cr–1%Al showed more protective behavior initially, but breakaway occurred at 1200°C (ODD′, ODE) and, to a lesser extent, at 1000°C (OHH′, OHI). The addition of 4.5%Al to Co–15%Cr led to a wide range of oxidation kinetics at 1200°C, typified by OBB′ and OBC at one extreme and OJK and OJJ′ at the other. At 1000°C, this alloy showed initially protective behavior (OJK), with some slight breakaway behavior occasionally being observed (OJJ′). Similarly, protective behavior was observed for Co–28%Cr–4.5%Al at both 1000 and 1200°C (OJK), although some slight breakaway did occur (OJJ′).

Fe–12.9%Cr–1.3%Al oxidized rapidly at 1200°C (curves PLL′, PLM), but showed more protective behavior at 1000°C (PST). Fe–26.1%Cr–0.9%Al oxidized more slowly than Fe–12.9%Cr–1.3%Al at 1200°C (PNN′, PNR), and at a similar rate at 1000°C (PST). The addition of 5.7% Al to Fe–11.5%Cr resulted in protective behavior at 1000°C (PU) and at 1200°C initially (PST), although some breakaway occurred at the higher temperature (PSS′). Fe–27.8%Cr–4.9%Al showed protective behavior at both 1200°C (PST) and at 1000°C (PU).

Ni–Cr–Al alloys containing 15 to 30% Cr and 1% Al yielded protective behavior at 1000 and 1200°C (curve QV), while those containing 15 to 30% Cr and 4 to 4.5% Al produced even more protective behavior at both temperatures (QW).

The main types of scales formed on these alloys, as shown schematically in Fig. 2, were:

1. α-Al_2O_3, containing 1 to 5% Cr and 0.5 to 1% of the basis metal M, (Fe, Ni, or Co), in solid solution.
2. Cr_2O_3, containing 1 to 5% Al and 0.5 to 1% M in solution, with a healing α-Al_2O_3 layer, containing some chromium and a little M in solution, at its base. The two layers interdiffused to some extent. Internal oxide of α-Al_2O_3 was present below such layers on Ni–Cr–Al and Co–Cr–Al alloys, but not on Fe–Cr–Al alloys. These double layers did not break away as easily as Cr_2O_3 or Al_2O_3 alone.
3. Cr_2O_3 containing 1 to 5% Al and 0.5 to 1% M in solution, with an internal oxide of α-Al_2O_3.
4. Thick nodules, formed after mechanical fracture of the initially

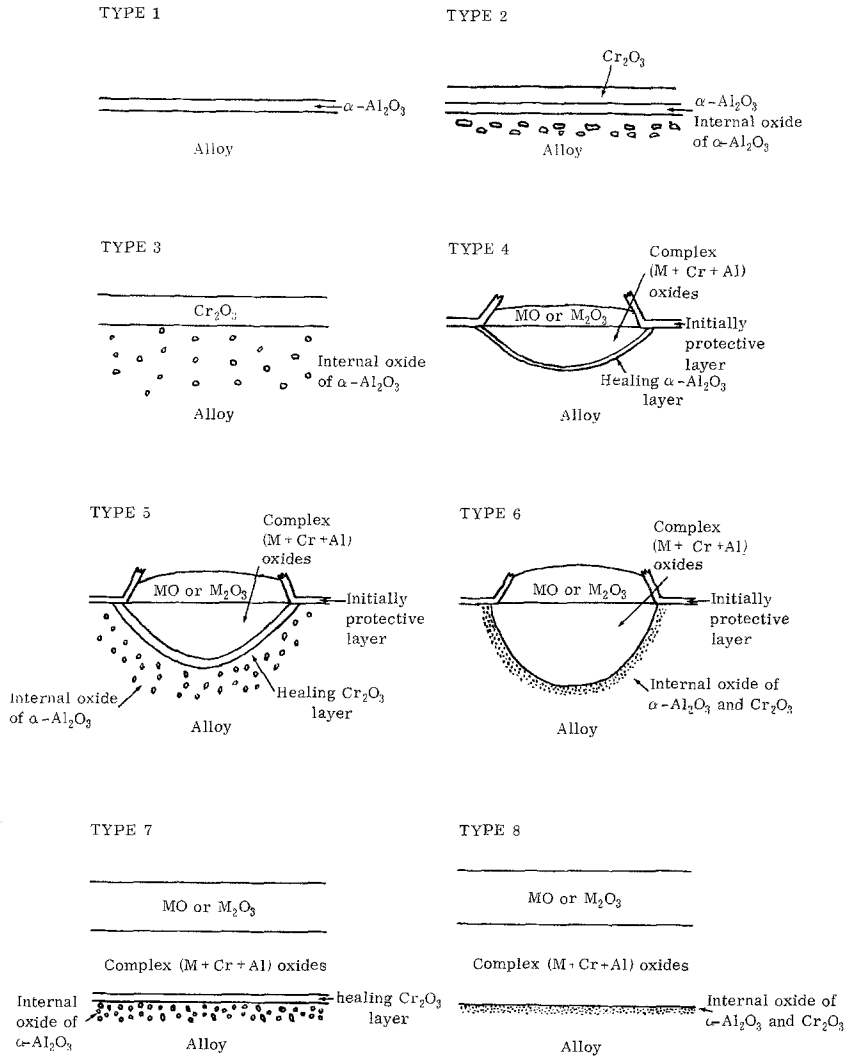

Fig. 2. Schematic diagrams of the morphology of scales formed on Co–Cr–Al, Fe–Cr–Al, and Ni–Cr–Al alloys. The actual sizes of the nodules and other features depend considerably on the alloys, the oxidation time, and the temperature.

protective layer, rich in MO (or M_2O_3 in the Fe–Cr–Al case), with an inner layer containing particles of spinel in an MO matrix, or a spinel layer, and a healing α-Al_2O_3 layer at the base.

5. As with 4, but with a healing layer of Cr_2O_3 and internal oxide particles of α-Al_2O_3.

6. As with 4, but no healing layer developed and internal oxide particles of α-Al_2O_3, with occasional Cr_2O_3 and even apparently α-Al_2O_3–Cr_2O_3 particles, were present.
7. Thick scales similar to 5, but which developed from the start of the run or very soon afterward.
8. Thick scales similar to 7, with no healing Cr_2O_3 layer but internal oxide of both α-Al_2O_3 and Cr_2O_3.

With scale 1, small amounts of MO or M_2O_3 and Cr_2O_3 were sometimes found outside the α-Al_2O_3, and with scales 2 and 3 small traces of MO or M_2O_3 could be found outside the main Cr_2O_3 layer. Possibly thin spinel layers had begun to develop at the interface between these outer residual layers and the main oxides. These outer layers were produced in the very early, transient scaling stages and are not considered in detail in the present paper.

Table II summarizes the main types of scale, although in some cases the situation has been simplified to enable comparisons to be made. Although the chromium and aluminum levels were not absolutely identical in the individual alloys, four main categories were apparent.

Table II. Comparison of the Types of Scale Formed on Fe–Cr–Al, Ni–Cr–Al, and Co–Cr–Al Alloys

Alloy composition (wt. %)	Type of scale	
	1000°C	1200°C
Fe–12.9Cr–1.3Al	Type 1 initially, followed by breakaway almost at once, especially at 1200°C, to give type 6 and to a lesser extent type 4	
Fe–26.1Cr–0.9Al	Type 2 (27% of surface) Type 3 (73% of surface)	Type 2 (5% of surface) Type 3 (95% of surface)
Ni–15.1Cr–1.1Al	Type 2 predominantly	Type 2 predominantly
Ni–28.8Cr–1.0Al	Type 2 predominantly	Type 2 predominantly
Co–10.0Cr–1.0Al	Type 8	Type 8
Co–15.0Cr–1.0Al	Type 8, becoming increasingly type 7 with time, especially at 1000°C	
Co–30.0Cr–1.0Al	Type 3, followed by type 5 after breakaway	
Fe–11.5Cr–5.7Al	Type 1	Type 1 initially, followed by some breakaway to give type 6 only
Fe–27.8Cr–4.9Al	Type 1	Type 1
Ni–14.8Cr–4.4Al	Type 1	Type 1
Ni–28.7Cr–4.3Al	Type 1	Type 1
Co–15.0Cr–4.5Al	Types 1, 2 and 7, with 1 and 2 predominating at 1000°C (and type 7 at 1200°C)	
Co–28.0Cr–4.5Al	Mainly type 1, some type 2, followed by breakaway in a few isolated areas to give rapidly healed type 4	

10–15% Cr and 0.9–1.3% Al

Additions of chromium and aluminum at these levels to iron gave an initial, protective α-Al_2O_3 layer which rapidly broke down, yielding iron-rich oxides, some of which were subsequently healed. Such additions to nickel, however, produced a protective scale of Cr_2O_3 with a healing α-Al_2O_3-rich layer below (Cr_2O_3–α-Al_2O_3). Cobalt alloys gave only non-protective cobalt-rich oxides, with minimal healing by Cr_2O_3 for higher chromium levels after longer times.

26–30% Cr and 0.9–1.3% Al

Such additions to iron gave protective layers of Cr_2O_3 or Cr_2O_3–α-Al_2O_3 and to nickel gave protective Cr_2O_3–α-Al_2O_3. Cobalt alloys, however, gave a protective Cr_2O_3 scale initially, which rapidly broke down to give cobalt-rich oxides, subsequently healed by Cr_2O_3.

10–15% Cr and 4.3–5.7% Al

Alloying at this level produced a mainly protective α-Al_2O_3 layer on Fe–Cr–Al, with some breakdown to give iron-rich oxides, especially at 1200°C. Although Ni–Cr–Al gave a protective α-Al_2O_3 layer in all cases, Co–Cr–Al yielded scales ranging from such α-Al_2O_3 layers and Cr_2O_3–α-Al_2O_3 double layers to thick cobalt-rich oxides, especially at 1200°C.

26–30% Cr and 4.3–5.7% Al

These high chromium and aluminum levels always produced α-Al_2O_3 scales on Fe–Cr–Al and Ni–Cr–Al alloys. With Co–Cr–Al alloys, however, although α-Al_2O_3 predominated, Cr_2O_3–α-Al_2O_3 and some breakdown to give cobalt-rich oxides rapidly healed by α-Al_2O_3 were also evident.

DISCUSSION

The ease of formation of protective α-Al_2O_3 on the alloys, and the lowest weight gain necessary to achieve this protective layer, are in the order Fe–Cr–Al > Ni–Cr–Al > Co–Cr–Al. On the other hand, where rapid scaling is liable to occur as a result of breakaway of protective α-Al_2O_3, Cr_2O_3, or Cr_2O_3–α-Al_2O_3 oxide layers, Ni–Cr–Al gives the most reliable protective scales. Co–Cr–Al produces nodular growths as a result of breakaway, or by growth from the outset of a run, most generally distributed over the alloy surface. Fe–Cr–Al gives less surface area which has undergone breakaway at a catastrophic rate. Thus, although for a given chromium and aluminum content the overall weight gain of the Co–Cr–Al alloy is greater

than that of the corresponding Fe–Cr–Al alloy, locally formed nodules on the Fe–Cr–Al alloy can grow considerably faster than on the Co–Cr–Al alloy. In all cases, breakaway is more prevalent, and tends to be more disastrous at 1200°C than 1000°C.

In discussing the reasons for these modes of behavior, it must be appreciated that few values of the pertinent alloy and oxide parameters exist for these ternary alloys, and it is necessary to rely upon analogy with the corresponding binary alloys and even pure metals.[3] It should, however, be remembered that the ternary nickel and cobalt alloys containing at least 4% Al are two-phase. In particular:

1. The alloy interdiffusion coefficient is an order of magnitude lower in fcc Ni–Cr alloys, and two orders of magnitude lower in Co–Cr alloys, than in the corresponding appropriate Fe–Cr alloys.
2. The oxygen diffusivity in iron is less than in nickel and, by analogy, probably than in cobalt.
3. The oxygen solubility is greater in nickel and cobalt than in iron, as far as the scanty data indicate.
4. The growth rates of FeO, CoO, NiO, Cr_2O_3, and α-Al_2O_3 (grown on Fe–Al alloys) are in the ratio $1:10^{-1}:10^{-3}:10^{-5}:10^{-6}$ to 10^{-7}. These differences are partly reduced in certain cases by doping effects.
5. The free energy of formation at the relevant temperatures has a larger negative value for FeO than for CoO, which itself has a slightly larger negative value than NiO.
6. Fe–Cr spinel has a wide range of composition, whereas Co–Cr spinel has a narrower range, and Ni–Cr spinel essentially has a fixed composition.
7. The stresses developed in α-Al_2O_3 and Cr_2O_3 layers formed on these alloys have never been measured and it is not known how they are affected by the minor doping constituents. Similarly, little is known about the plasticity or creep of the scales and their substrates, or of the fracture characteristics of the oxides. Perusal of the general ceramics literature[1] indicates that the strength of Al_2O_3 is increased by additions of M, with chromium having the greatest effect, followed by iron, cobalt, and finally, nickel. Consequently perhaps Al_2O_3 on Fe–Cr–Al is least likely to deform, but also least likely to fracture at a given stress level. However, this argument cannot be pressed very strongly in considering the complicated scaling situation.

The oxidation mechanism of the alloys is evidently as follows. Upon immediate exposure to oxygen at temperature, the surfaces are covered by nuclei of MO, M_2O_3, Cr_2O_3, Al_2O_3 and probably spinels, so the effective oxygen partial pressure or potential at the alloy–oxide interface is now

lowered considerably. This enables preferential oxidation to occur. The processes after this stage depend upon the alloy composition.

10–15% Cr and 0.9–1.3% Al

The effect of aluminum is to "getter" oxygen, forming α-Al_2O_3. In the Ni–Cr–Al case, where the effective oxygen partial pressure at the alloy–oxide interface and the oxygen solubility and diffusivity in the alloy are relatively high, and the alloy interdiffusion coefficient is low, this occurs to some depth in the alloy initially, giving internal oxide. Although some chromium is then permitted to react with any residual dissolved oxygen to form more internal oxide, much of it can diffuse to the surface to form a complete layer, rich in Cr_2O_3. The low effective oxygen pressure below this Cr_2O_3 layer, which is of low dissociation pressure, now causes the inward flux of oxygen to be reduced. Internal oxide particles rich in α-Al_2O_3 can then grow laterally, linking up to give a complete layer at the Cr_2O_3–alloy interface.

With Fe–Cr–Al alloys the dissociation pressures of FeO and Fe_3O_4 are lower than that of NiO, and the diffusivity and solubility of oxygen in the alloy are smaller than in Ni–Cr–Al. These factors, together with the relatively high alloy interdiffusion coefficient in the alloy, enable aluminum to produce a complete layer of α-Al_2O_3 at the alloy surface very rapidly. The chromium probably assists in the formation of Al_2O_3 by "gettering" oxygen to some extent at the surface in the initial stages.

In the Co–Cr–Al case, the probable relatively high oxygen solubility and diffusivity in the alloy, together with the low alloy interdiffusion coefficient, require α-Al_2O_3 to form as an internal oxide, rather than as a surface layer. As for Ni–Cr–Al, this enables some chromium to react with the diminished oxygen in the alloy to give further internal oxide. However, CoO grows much more rapidly than NiO and is able to overgrow and undercut the other nuclei, incorporating them into the scale before a Cr_2O_3–α-Al_2O_3 layer can form. This CoO-rich scale grows very rapidly, as the parameter values stated above indicate, and prevents formation of a healing layer, at least until the growth rate slows substantially (as with Co–15Cr–1Al).

Lifting and cracking open of the protective scale of Cr_2O_3–α-Al_2O_3 on Ni–Cr–Al are not readily achieved because the adhesion of the oxide is good, due to the internal oxide and subscale loops which develop and key the scale to the alloy. Breakaway of the α-Al_2O_3 scale formed on Fe–Cr–Al occurs more readily. This is probably at least partly due to the more rapid diffusion of aluminum in the alloy than in the oxide, producing a smooth alloy–oxide interface, so causing little mechanical "keying-on" of the oxide. When fracture does occur, very fast oxidation of the depleted alloy immediately exposed to the hot gas can occur and persist. The population of internal oxide

particles produced is not always sufficiently dense to allow linking to form a healing layer at the scale base, so these are quickly overgrown due to the very rapid encroachment rate of iron oxides on the alloy. As the Fe–Cr spinel has a wide composition range, it is, however, possible that iron-rich, chromium-rich, and even aluminum-rich nuclei can form a spinel layer, which helps to slow down this rapid breakaway oxidation to some extent. It is possible to conceive of situations on certain alloys, particularly after long oxidation times, where complete layers of protective nickel-containing or cobalt-containing spinels are formed and exert important influences, but no direct evidence of their existence or influence was detected in the present work. The high metal interdiffusion rate and low oxygen solubility and diffusivity in the Fe–Cr–Al alloy also assist in forming healing layers at the base of such iron-rich nodules.

26–30% Cr and 0.9–1.3% Al

For the Fe–Cr–Al and Ni–Cr–Al alloys, the higher chromium contents and slightly lower aluminum contents than with the previous systems result in the protective layers being richer in chromium than previously. The alloy interdiffusion coefficient may also differ slightly between the systems, although no data are available. In both cases, the aluminum "getters" oxygen to form internal oxide, allowing chromium to diffuse to the surface to form a layer rich in Cr_2O_3. With Ni–Cr–Al, the internal oxide eventually develops laterally to form a layer rich in α-Al_2O_3 at the alloy–Cr_2O_3 interface. However, with Fe–Cr–Al, this only occurs in some areas, in others the protective layer remaining as Cr_2O_3 alone, with internal oxide of α-Al_2O_3. The aluminum and chromium contents of the actual Fe–Cr–Al alloy studied were slightly lower than those of the Ni–Cr–Al alloy. Furthermore, the Fe–Cr–Al alloy was oxidized exclusively in oxygen saturated with the volatile species from Cr_2O_3, which may have influenced the nature of the scales produced.

With Co–Cr–Al, many rapidly growing, initial, cobalt-rich nuclei are able to form on the alloy surface. This results in a relatively high effective oxygen pressure at the alloy surface. The aluminum "getters" oxygen to form α-Al_2O_3 internal oxide and chromium diffuses to the alloy surface to form a complete layer of Cr_2O_3. The probable high oxygen solubility and diffusivity in the alloy and the low alloy interdiffusion coefficient result in the alloy next to the Cr_2O_3 being depleted in chromium and aluminum. Thus, if the oxide lifts and fractures, cobalt-rich oxides can grow rapidly before a rehealing Cr_2O_3 layer can form. In practice, this happens very quickly after the initial Cr_2O_3 layer has formed, preventing any possible development of α-Al_2O_3 layers.

10–15% Cr and 4.3–5.7% Al

For the Fe–Cr–Al and Ni–Cr–Al alloys, these additions are sufficient to enable an external layer of α-Al_2O_3 to form. These layers are liable to fracture at temperature for the previously outlined reasons. With Ni–Cr–Al, where the growth rate of NiO is slow, rehealing by α-Al_2O_3 can occur without any significant increases in weight occurring. However, as the growth rates of FeO and Fe_3O_4 are very rapid, failure of the α-Al_2O_3 results in some breakaway behavior, with iron-rich oxides forming and consequent difficulty or impossibility in reestablishing healing layers of α-Al_2O_3, or even Cr_2O_3.

With Co–Cr–Al, several different scales form on different parts of the specimen surface, due to local variations in conditions and properties. The supposed high solubility and diffusivity of oxygen in the alloy and the low alloy interdiffusion coefficient, together with the rapid growth of CoO, enable some areas to develop CoO-rich scale. However, in others α-Al_2O_3 or Cr_2O_3–α-Al_2O_3 layers form on the surface due to the high bulk aluminum and chromium contents.

26–30% Cr and 4.3–5.7% Al

With all three materials, there is sufficient chromium and aluminum to permit external α-Al_2O_3 to form. Chromium can act as a "getter" for oxygen in the initial stages. If lifting and fracture of this layer does occur, the slow growth rate of NiO in the Ni–Cr–Al case, and the rapid interdiffusion rate in the Fe-Cr-Al case, allow rehealing to occur before any significant amounts of M-rich oxides can form. Only on the Co–Cr–Al alloy, where the alloy interdiffusion coefficient is low, and the growth rate of CoO high, do any substantial breakaway regions develop. Even in this case, the CoO-rich scales are readily rehealed by α-Al_2O_3.

ACKNOWLEDGMENTS

The authors thank Professor T. K. Ross for providing facilities and Mr. B. W. Lambert for his collaboration with the electron probe microanalysis. Two of the authors (F.H.S. and M.G.H.) are grateful for financial support from the Science Research Council and the Ministry of Defence (Admiralty) within the period 1963–1970 when the work was conducted.

REFERENCES

1. F. H. Stott, Ph.D. Thesis, University of Manchester (1970).
2. M. G. Hobby, M.Sc. Thesis, University of Manchester (1968).
3. B. Chattopadhyay and G. C. Wood, *Oxidation of Metals* **2**, 373 (1970).